Pergamon

Journal of Structural Geology, Vol. 20, No. 11, pp. 1477 to 1493, 1998

PII: S0191-8141(98)00048-0

0191-8141/98 $ - see front matter

Linkage and evolution of conjugate strike-slip fault zones in limestones of Somerset and Northumbria

P. G. KELLY* and D. J. SANDERSON

Geomechanics Research Group, School of Ocean and Earth Science, University of Southampton, Southampton Oceanography Centre, Southampton, SO14 3ZH, U.K.

and

D. C. P. PEACOCK

Rock Deformation Research Group, School of Earth Sciences, University of Leeds, Leeds, LS2 9JT, U.K.

(*Received* 3 *June* 1997; *accepted in revised form* 1 *May* 1998)

Abstract—Conjugate strike-slip fault zones that cover metre-scale areas at Beadnell, Northumbria, and Kilve, Somerset, were initiated as conjugate vein arrays. Early conjugate faults are linked by the propagation of one fault that eventually by-passes the other fault. A model for the development of strike-slip faults is presented, using fault and vein geometries and the position of damage zones with respect to the master faults as an indication of the propagation direction. This model includes the evolution of networks from (1) the initial random development of vein arrays, to (2) the isolated development of several unconnected conjugate fault segments that pass into vein arrays, through (3) the intersection of a conjugate set of master faults and linkage with minor antithetic faults, and the formation of new vein arrays with extensional geometries after a linked network of faults is established, to (4) breaching of intersection points by dominant faults, and finally (5) the propagation towards oversteps that are breached to form a through-going fault. The geometry of the active structures simplifies with time, as strain is localised along the master fault, but the complexities are preserved in the fault walls.

INTRODUCTION

Damage zones consist of small faults and veins (*subsidiary fractures*) in the vicinity of larger structures (*master faults*) (Chester and Logan, 1986). Such zones are often related to the propagation of the larger fault (Scholz *et al.*, 1993; Reches and Lockner, 1994) and processes at fault-tips (McGrath and Davison, 1995). In particular, Reches and Lockner (1994) identify a process zone, during experimental fracture of Western Granite, consisting of an area of extensional (Mode 1) fracture at the fault-tip that enhances propagation (Fig. 1). The process zone moves with the fault-tip, leaving damaged rock in its wake (Scholz *et al.*, 1993). The process zone is asymmetric about a Mode II tip, reflecting the propagation direction and sense, and controls the location and width of the damage zone. Zones of 'damaged' rock adjacent to faults may also arise from structures that form prior to the development of a through-going fault. Cowie and Scholz (1992) demonstrate how a planar fault develops from arrays of fractures that coalesce to form an irregular fault plane. The asperities are by-passed during displacement accumulation, leading to the formation of a smooth fault plane. On the metre-scale, strike-slip relay ramps (Peacock and Sanderson, 1995a) form in contractional zones in between overstepping strike-slip fault segments. In their model, a smooth fault plane with a contractional bend develops after the relay ramp has been breached, and the inactive parts of the structure are preserved adjacent to the fault.

The location and geometry of damage zones are important as they may contribute to the compartmentalisation, or provide fracture-controlled fluid flow pathways in addition to the master fault in a reservoir (e.g. Knott *et al.*, 1996). The development of strike-slip fault zones is of interest in permeability studies, as it will be demonstrated that these faults develop initially in isolation, and linkage of fractures may occur during later evolution.

The aim of this paper is to show how the development of conjugate strike-slip faults in limestones, over scales of millimetres to tens of metres, may be described with a common fault evolution model. The formulation of the model is based on field observations at two locations: Kilve, Somerset, and Beadnell, Northumbria (Fig. 2). The justification of using two locations and several examples, is based on the range of comparable structures in both areas.

The mechanics of conjugate fault development have been the subject of much debate, with particular emphasis on the nature of the intersection or offset of the conjugate sets. For example, Freund (1974), using analogue modelling, identifies geometrical impossibilities prohibiting intersecting conjugate faults from

*E-mail address: Paul.Kelly@soc.soton.ac.uk

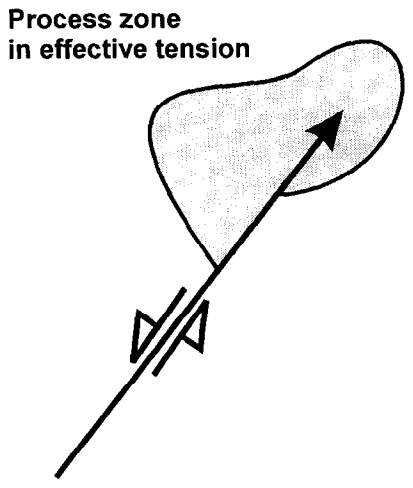

Fig. 1. The location of a zone of effective tension at the tip of a right-propagating sinistral fault containing tensile microcracks (Reches and Lockner, 1994). The process zone moves with the propagating fault, and coalescence of the microcracks influences the position of the damage zone (Scholz *et al.*, 1993).

being displaced synchronously, but Nicol *et al.* (1995) interpret normal fault geometries on seismic sections from the Timor Sea and conclude that synchronous movement on conjugate sets is possible (cf. sandbox modelling of Horsfield, 1980). Odonne and Massonnat (1992a) model conjugate fractures in paraffin wax and show that an inequality in either length or orientation to the major principal strain axis of one of the conjugate pair can lead to offset of the other, even during synchronous development. High strain areas in the acute angle adjacent to a stuck intersection (Peacock, 1991; Nicol *et al.*, 1995) may cause volume loss through pressure solution during synchronous movement (Odonne and Massonnat, 1992b).

Central to the comparison of the structures at both locations is the occurrence in the conjugate strike-slip fault zones of arrays of échelon veins (Fig. 3). Several classifications and mechanical models have been proposed for échelon vein array formation. Beach (1975) sub-divided conjugate vein arrays into two categories, Type 1 and Type 2 (Fig. 4). Type 1 vein arrays have convergent vein geometries, whereby the veins in one conjugate set are parallel to the zone boundary of the other set (Fig. 4a). Type 2 veins are sub-parallel to the bisector of conjugate dextral and sinistral arrays (Fig. 4b). For the purposes of this study the Type 1 and Type 2 classifications (Fig. 4) are adopted as strictly geometrical descriptive terms, and do not refer to the mode of formation of the vein arrays. Pollard *et al.* (1982) observe that échelon fractures form at the tips of parent cracks, and their orientations reflect the remote stress system. Rothery (1988) classified extensional and shear arrays based on the angle between the vein strike and the array orientation (the vein-zone angle), as there was inconclusive evidence regarding the array formation. Extensional arrays have vein-zone angles of <27 , whilst the vein-zone angles in shear arrays are >27 (Rothery, 1988). Olson and Pollard (1991) use numerical modelling to show veins may develop at angles to the array ranging from 0 to 55 in a purely extensional environment. In their models, sub-parallel microcracks initiate, independently of localised shear or a parent fracture, from randomly distributed flaws in the rock. Growth of the microcracks is dependent on the extent of interaction with adjacent cracks, leading to a range of apparently extensional to shear vein array geometries (Olson and Pollard, 1991).

Gamond (1983) and Peacock and Sanderson (1995b) demonstrate how vein arrays evolve into pull-apart arrays through dilation of the veins between overstepping 'P'-shears (Fig. 3b) that may be eventually faulted (Fig. 3c) (Cowie and Scholz, 1992). Pull-aparts occur in dilational jogs between overstepping shear fractures (Sibson, 1989) over several orders of magnitude (Aydin and Nur, 1982), from the millimetre-scale (Peacock and Sanderson, 1995b), to sedimentary basins on the kilometre-scale (e.g. Hempton and Dunne, 1984). A dilational jog occurs between either right-stepping dextral faults or left-stepping sinistral faults (Segall and Pollard, 1980), and may also occur during movement at a releasing bend found at the intersection point of oblique fault segments (Mann *et al.*, 1983; Sibson, 1989).

For the purposes of the metre-scale maps, the master faults are those that define the triangles of the conjugate sets, are relatively through-going, and have larger displacements (>100 mm in the examples mapped). The subsidiary fractures are the smaller displacement faults and veins adjacent to the master faults. The offset of earlier faults and veins, the length of pull-aparts, and the strike-separation of faulted pull-aparts may all be used to estimate fault displacements (Peacock and Sanderson, 1995b). It is easier to measure the displacements on the subsidiary fractures within the zones, as the pull-aparts are generally well preserved.

To investigate the formation of conjugate strike-slip faults in limestones, metre-scale examples are described in this paper that have been mapped at a scale of 1:25, using a grid drawn on the rock. The discussion of conjugate strike-slip fault zone formation at Beadnell is founded on kinematic analysis of vein and pull-apart arrays. A network of conjugate strike-slip faults exposed at Kilve over an area approximately 350×200 m, and mapped at a scale of approximately 1:500 onto aerial photographs provided the opportunity to study fault geometry and linkage at a larger scale. The development of conjugate fault zones, at both Kilve and Beadnell, has been assessed through the appraisal of vein array geometries, fault propagation direction using the asymmetric distribution of fracture density adjacent to the faults (cf. Scholz *et al.*, 1993; Reches and Lockner, 1994), and the modified displacement-gradient tensor method of strain analysis

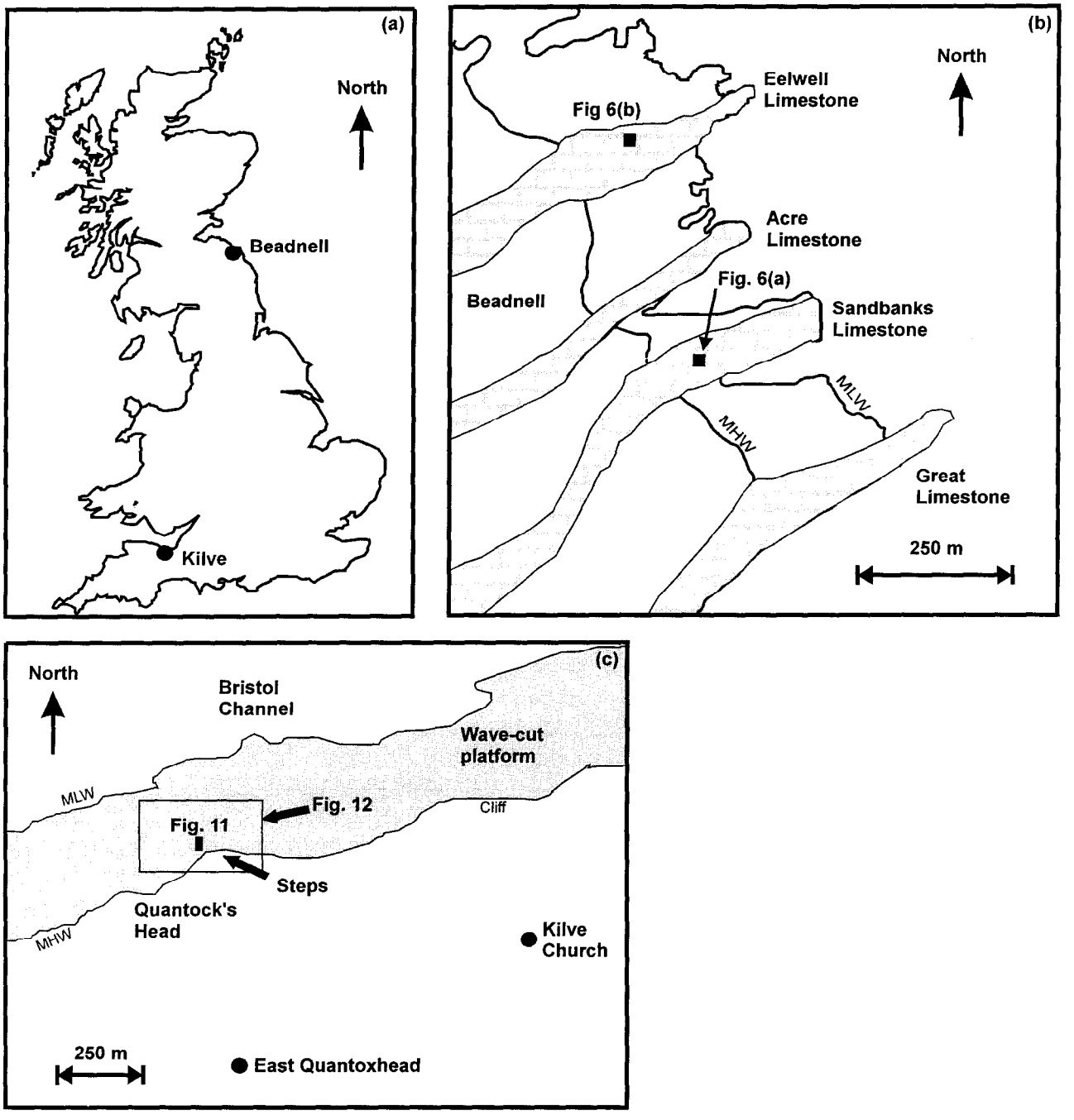

Fig. 2. (a) Map of part of the British Isles showing the locations of (b) Beadnell, Northumbria, and (c) Kilve, Somerset. The locations of the strike-slip fault zones described in the text are also shown. MHW = mean high water, and MLW = mean low water.

(Jamison, 1989; Peacock and Sanderson, 1993). In conclusion, a conjugate strike-slip fault zone evolution model has been developed by combining the observations at both localities.

STRIKE-SLIP FAULTS AT BEADNELL, NORTHUMBRIA, U.K.

There are good examples of metre-scale conjugate strike-slip fault zones on the upper bedding surfaces of Lower Carboniferous limestones that dip gently southeast. The faults are conjugate about an approximately east–west horizontal compressive axis and are associated with N–S-trending anticlines and millimetre-scale displacement thrusts that link the master strike-slip faults (Fig. 5) (cf. Shiells, 1964). Folds and thrusts are generally absent in the unfaulted regions. Structural maps of the Sandbanks and Eelwell Limestone surfaces drawn by Shiells (1964, figs 7 and 9) are extremely detailed, although fault displacements were not constrained. The maps show clearly that the strike-slip

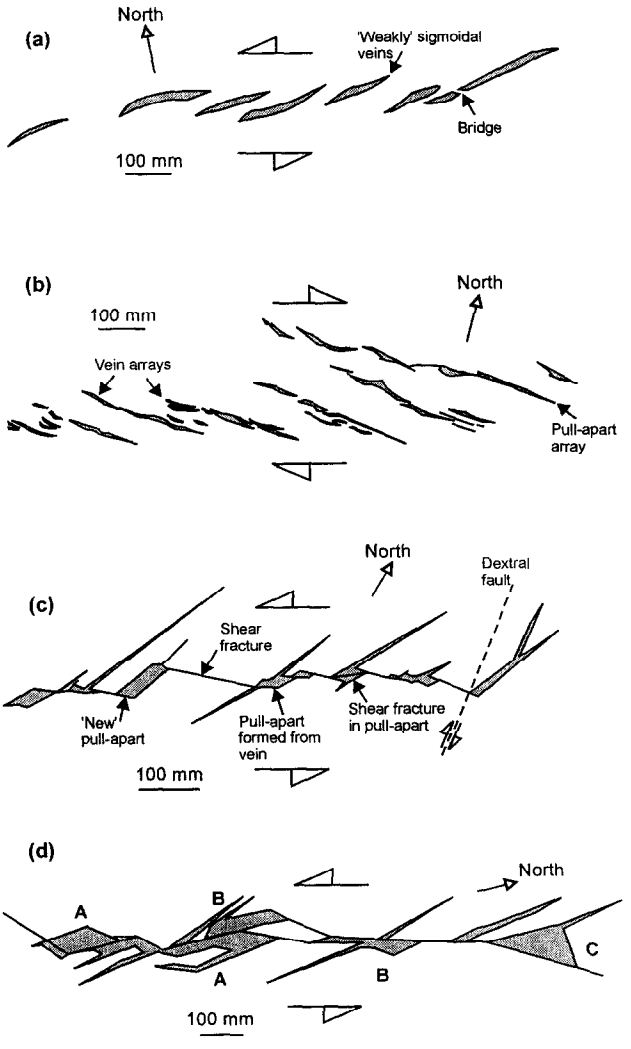

Fig. 3. Field examples from Beadnell and Kilve of (a) and (b) vein array, (c) a pull-apart array, and (d) a strike-slip fault with sheared calcite-filled pull-aparts adjacent to the faults.

faults are highly clustered and concentrated in almost linear zones. In between the fault zones, vein arrays (termed tension gash échelons by Shiells, 1964) are conjugate about an east–west axis. The majority of the veins are straight, but there are examples of slightly sigmoidal veins. Rare examples of fibres within the veins are sub-perpendicular to the vein walls, indicating Mode I opening. Shiells (1964) noted that the vein arrays are not only conjugate to each other, but also to the strike-slip faults. The strike-slip faults at Beadnell occurred as a result of approximately east–west compression during the Variscan Orogeny (Shiells, 1964; Collier, 1989), that also caused N–S-trending folds (Benard *et al.*, 1990). The compressional phase is sandwiched between two extensional phases that affected northeast England (Collier, 1989). The ENE–WSW- to NE–SW-striking normal faults were initiated in the Late Devonian (Shiells, 1964) and ceased during the Early Carboniferous (Collier, 1989). The Whin Dykes were intruded and some of the ENE–WSW normal faults were reactivated during post-compressional extension in the Permian (Robson, 1977; Collier, 1989). The fault traces are exposed on the surfaces of limestone units, but their three-dimensional geometries are more difficult to observe.

The fault zone shown in Fig. 6(a) contains strike-slip faults associated with veins and pull-apart arrays. Veins oblique to the strike of the faults are common, and usually terminate at the fault. The maximum fault displacement, measured parallel to a fault, is 225 mm. The faults are irregular, and fault segments often terminate or link at contractional or dilational oversteps. The master fault planes do not link to form a through-going network of faults (i.e. a percolating cluster, Stauffer and Aharony, 1992), but terminate in the rock and are co-linear with arrays of veins and pull-aparts. The majority of the arrays form conjugate sets and have convergent vein geometries (Type 1, Beach, 1975) where the veins in one conjugate set parallel the zone boundary of the other conjugate set. There are some examples of bisector-parallel veins close to the termin-

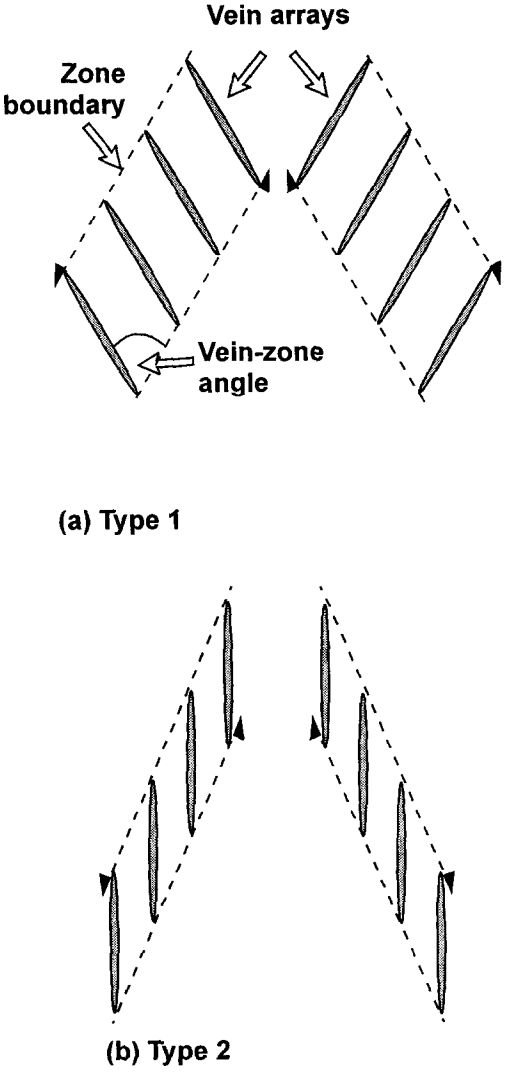

Fig. 4. Schematic diagrams of convergent (Type 1) vein arrays, and bisector parallel veins (Type 2) (Beach, 1975).

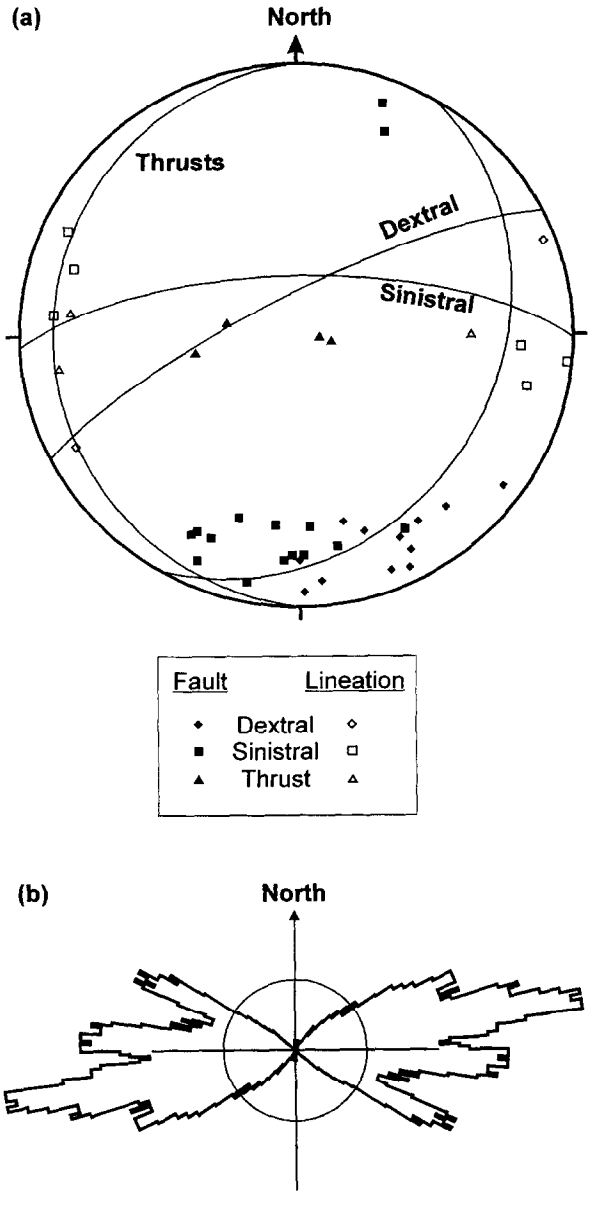

Fig. 5. Data from the mapped fault zones at Beadnell, Northumbria. (a) Equal-area stereogram of poles to planes of sinistral (n = 15) and dextral (n = 11) strike-slip faults, and of thrusts (n = 4). Lineation data and synoptic great circles for the faults are also shown. (b) Rose diagram of the vein array orientations within these fault zones (n = 100). The data can be divided into three groups based on orientations: (i) NW–SE, (ii) ENE–WSW and (iii) ≈E–W. The first two form a conjugate set of arrays, with a sinistral NW–SE group and a dextral ENE–WSW group.

ations of master faults (Type 2, Beach, 1975). Thrusts with millimetre-scale displacements link with the strike-slip faults and, in some instances, are offset and matchable across the strike-slip faults. There are, however, rare examples of thrusts that terminate at strike-slip faults.

A second example from Beadnell is of a much more linked network (Fig. 6b). The maximum fault displacement is approximately 500 mm, and the master faults have much more continuous traces than in the first example (Fig. 6a). Sheared pull-apart structures (Fig. 3c) occur along-side some of the faults, and there are examples of fault segments that overstep at dilational jogs. The largest faults link mainly by fault-tips abutting fault walls (tip–wall linkage), and there are no vein arrays that are co-linear with the faults. Damage between the largest faults consists of networks of clustered vein arrays and subsidiary faults with millimetre-scale displacements. The majority of the veins are sub-parallel to the acute bisector angle of the conjugate master fault traces (Type 2, Beach, 1975), with few exceptions. A N–S-striking dextral strike-slip fault offsets the northern conjugate set, indicating a later stage of deformation (at A, Fig. 6b).

Kinematic analysis

The kinematic evolution of the veins and pull-apart arrays in the fault zone maps can be determined using the construction of McCoss (1986), to find the relative infinitesimal wall-rock displacement direction (Fig. 7). Graphs of zone boundary orientation plotted against the strike of the veins within the arrays show major differences in the vein-zone angle for each of these two maps (Fig. 7a). In the map of unconnected faults there is a greater proportion of simple shear arrays (Fig. 6a) that plot in two clusters, one dextral and the other sinistral (Fig. 7a). The vein and pull-apart arrays from the connected network of strike-slip faults (Fig. 6b) plot in one cluster centred on the line of extension (Fig. 7a). In sharp contrast to the arrays in the unconnected strike-slip network (Fig. 6a), the majority of the transtensional arrays in the connected network (Fig. 6b) have a predominantly extensional component (Fig. 7a–c).

The displacement directions and extension and contraction axes are plotted onto maps of the master faults (Fig. 8). The vein arrays with simple shear geometries in the unconnected example imply displacement directions that are sub-parallel within linear zones, and reflect the displacement sense on co-linear strike-slip faults (Fig. 8a). The wall-rock displacement direction indicated by the vein arrays with transtensional geometries in the connected network of strike-slip faults illustrated in Fig. 8(b) are sub-perpendicular to the conjugate dihedral angle bisector orientation for the master fault traces. Therefore there is a marked contrast in the nature of veining in the two fault zones, with linear arrangements of simple shear arrays dominating the unconnected network, and clustered transtensional arrays dominating the connected fault zone. The significance of these observations is discussed fully in the Fault Evolution section below.

STRIKE-SLIP FAULTS AT KILVE, SOMERSET, U.K.

Lower Liassic rocks striking east–west are exposed in cliffs and on a wave-cut platform, and consist of

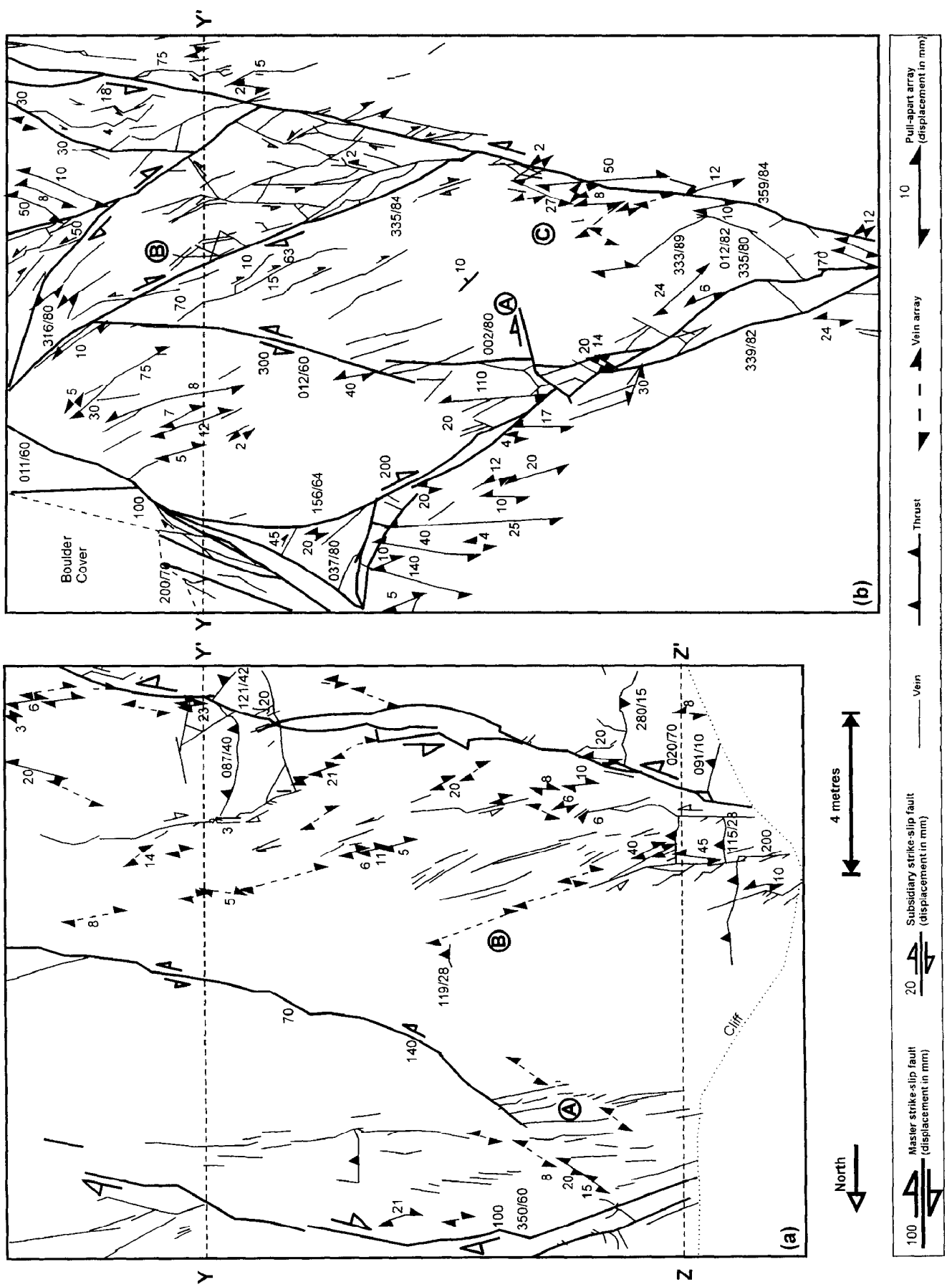

Fig. 6. Conjugate strike-slip fault zones mapped at Beadnell at a scale of 1:25. Displacements are in mm. The circled letters are referred to in the text. For location see Fig. 2(b). (a) Fault zone showing a conjugate arrangement of strike-slip faults that have not linked to form a network. (b) Network of linked strike-slip faults.

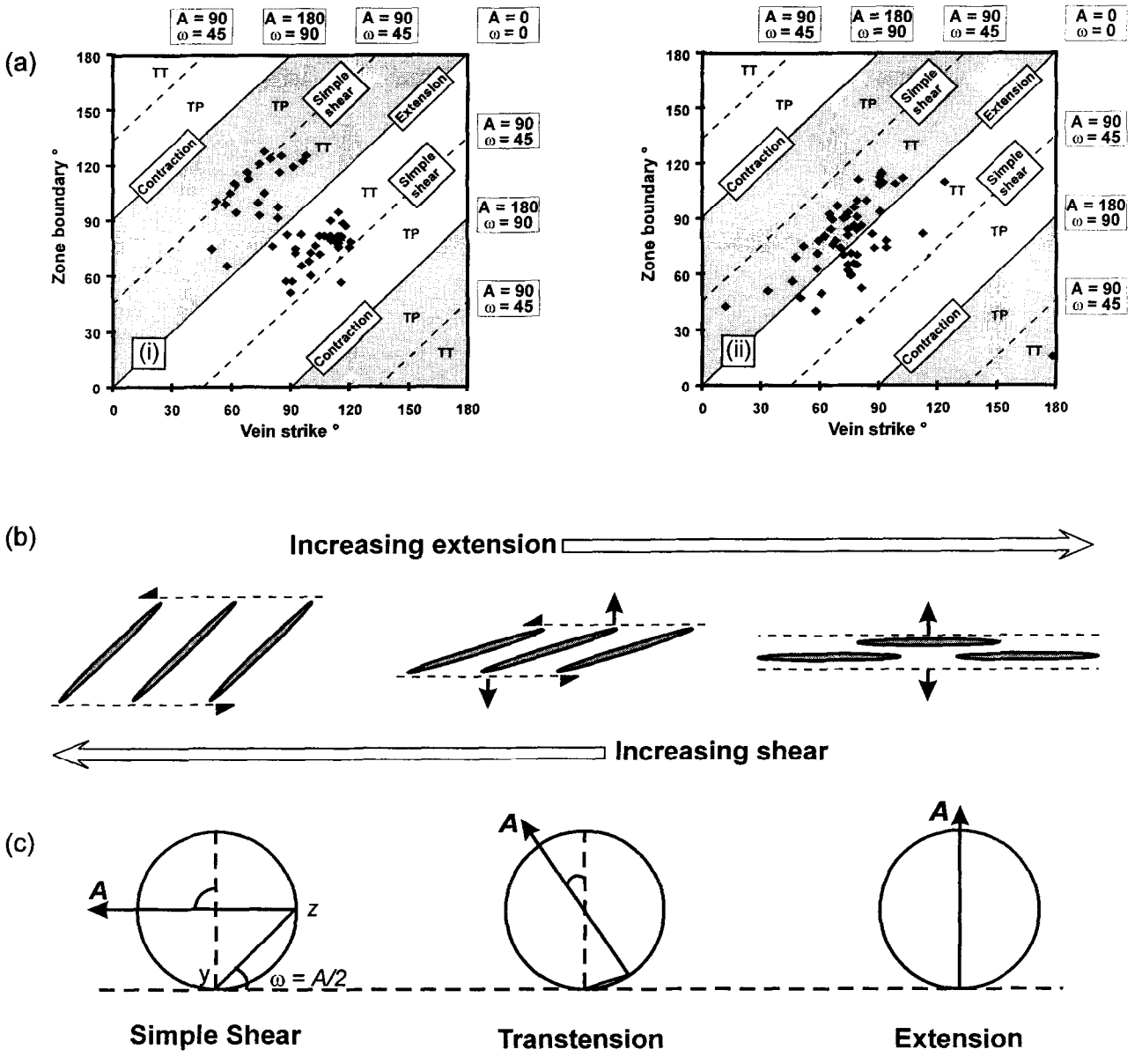

Fig. 7. (a) Graphs of zone boundary orientation and vein orientation to show the distribution of vein array geometries from Fig. 6. When the infinitesimal wall-rock displacement direction (A) is equal to the angle between the vein array and zone boundary (ω), the vein array has an extensional geometry. A difference of 90° signifies contraction, and one of 45° indicates that the array has a simple shear geometry. The lines of extension and contraction separate zones of dextral and sinistral displacement sense. The shaded areas indicate sinistral sense. TT = transtension; TP = transpression. (i) Data from Fig. 6(a), $n = 56$. The two distinct clusters of data indicate conjugate vein arrays that have predominantly simple shear geometries. (ii) Data from Fig. 6(b), $n = 60$. The single data cluster, centred on the extensional zone of the graph, demonstrates that the vein arrays in this fault zone have transtensional geometries, but are dominated by extension. (b) Schematic diagram of vein arrays with simple shear, transtensional and extensional geometries. (c) The construction of McCoss (1986) for each of vein arrays in (b). This method treats each vein array as a transtensional or transpressional zone (Sanderson and Marchini, 1984), to determine the infinitesimal displacement direction (A) of the wall-rocks from the zone boundary and the vein angle. A line parallel to the veins is drawn from point y to the circumference of a circle, z, that touches the zone boundary. A second line is drawn from z that passes through the centre of the circle, to find A.

limestones with thicknesses ranging from tens of millimetres to a maximum of about 0.5 m, interbedded with shales and mudstones up to 4 m thick. Strike-slip faults exposed in the cliff have slip lineations that pitch in the range 2–23°. In cross-section (Fig. 9) these strike-slip faults are not simple, steeply dipping planar structures but have bends and oversteps, and many of the strike-slip faults steepen through the more brittle limestone layers and shallow through the shale horizons, in a manner similar to normal faults in cross-section (Peacock and Zhang, 1994). This may indicate that the faults initiated as steep shear fractures in the more brittle limestone units, and the shallower dips represent either (1) up- or down-dip refraction of a

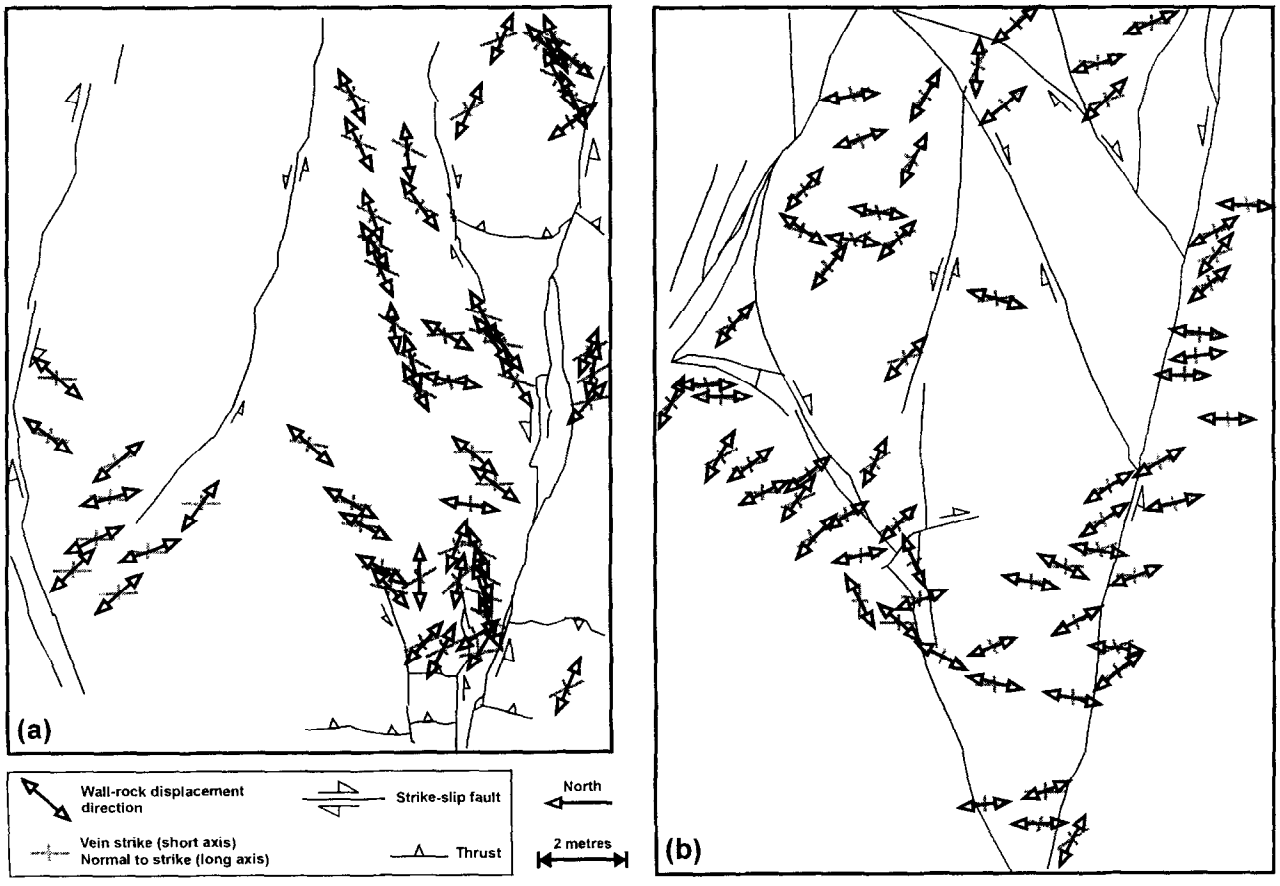

Fig. 8. Maps of the wall-rock displacement directions from vein systems (double-headed arrows). Extension (long axis of cross) and contraction (short axis) orientations are superimposed on maps of the master faults from Fig. 6. (a) The unconnected network which is dominated by co-linear vein arrays with simple shear geometries, and (b) the connected network, where transtensional vein arrays have predominantly extensional geometries.

propagating fault into the more ductile shale beds, or (2) linking faults between two overlapping segments, similar in style to the normal fault models described by Peacock and Sanderson (1992). The faults with normal components of displacement have the most complex geometries in cross-section (Fig. 9). Similarities between normal and strike-slip fault cross-sectional geometries may have important implications

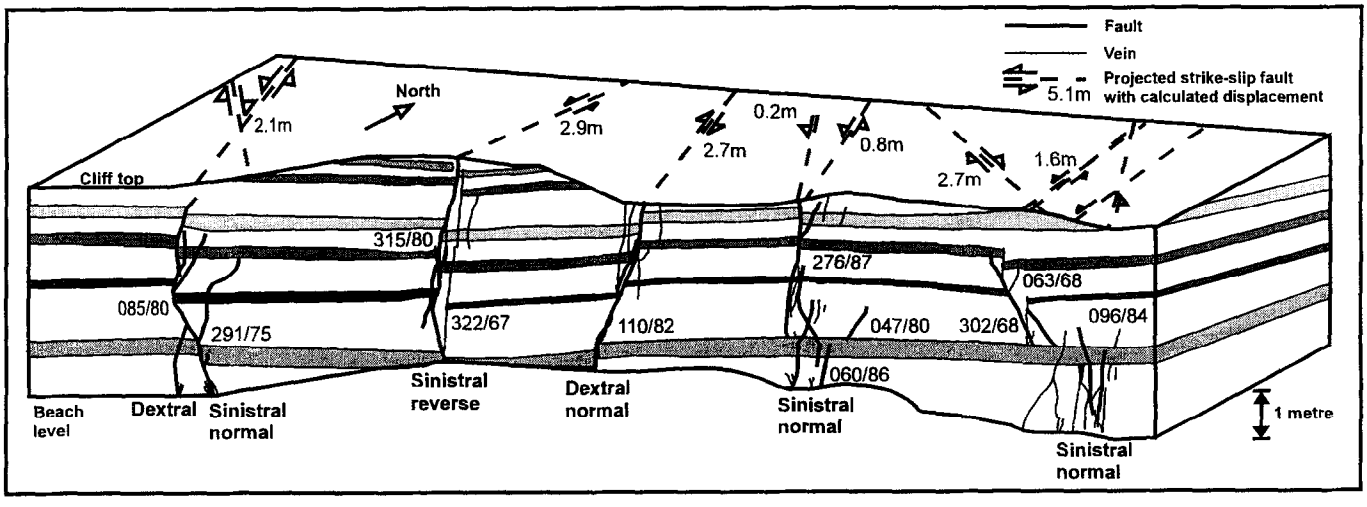

Fig. 9. Block-diagram of the strike-slip faults which exhibit a wide range of geometries in the cliff. Measured orientations of the strike-slip faults have been used to construct the plan (dashed lines) of the strike-slip faults on top of the cliff. The lateral displacements have been calculated using the trigonometric relationship between the slickenside lineation pitch and the vertical separation of beds. The shaded horizons represent individual limestone beds.

for fault movement analysis in seismic section interpretation.

On the wave-cut platform, the sinistral faults have N40°E strikes, whilst the dextral faults generally strike north–south (Fig. 10), and are evident at trace length scales from <1 m to >100 m (Figs 11 & 12). The average acute angle bisector of the fault traces has an orientation of N19°E. Palaeostress analysis using the *P–T* dihedra method, based on fault plane orientation and lineation data (Angelier, 1984), suggests that the maximum principal stress axis was approximately horizontal and NNE-trending during strike-slip fault formation. The minimum principal stress axis was horizontal and ESE-trending. Cross-cutting relationships indicate that the strike-slip faults post-date Mesozoic E–W-striking normal faults (Chadwick, 1986; Brooks *et al.*, 1988; Peacock and Sanderson, 1991; Bowyer and Kelly, 1995). The Cretaceous to Tertiary contraction responsible for the formation of the conjugate strike-slip faults also caused reverse reactivation on the east–west normal faults (Lake and Karner, 1987; Whittaker and Green, 1983; Peacock and Sanderson, 1992; Bowyer and Kelly, 1995).

Metre-scale examples

The example in Fig. 11 shows a through-going dextral fault that is comparable in style to the master sinistral fault in the connected fault network at Beadnell (Fig. 6b). There are conjugate sets of faults with millimetre-scale displacement adjacent to both of these master faults along which strain is localised (Figs 6 & 11). The breached intersection point in Fig. 11 is the major difference between these two examples. The intersection (at A, Fig. 11) of the master sinistral and dextral faults has been breached first by the sinistral fault, which in turn is displaced by a dextral fault that extends for approximately 50 m past the intersection point. The maximum strike-slip separation of a marker bed measured on the dextral fault is 3.5 m. A branch of the dextral fault by-passes the conjugate intersection, and linkage between the two branches is achieved through antithetic faults. Pull-apart arrays are rare, but do occur in these zones and faulted examples preserved along the length of the faults indicate their existence prior to through-fault development. On the inside of a bend on the main dextral fault at the northern end of the map, a network of conjugate subsidiary faults and pull-apart arrays occurs.

Exposure-scale strike-slip fault network

The strike-slip fault network exposed on the foreshore was mapped onto a base-map composed of aerial photographs, at a scale of approximately 1:500 (Fig. 12). On this scale, early sinistral faults are displaced by dextral faults that are themselves displaced by later sinistral faults formed between the larger, earlier sinistral strike-slips. The later sinistral linking faults have a more easterly strike than the earlier ones, and occur on the western side of the area (Fig. 12). Features present include oversteps and strike-slip relay ramps (Peacock and Sanderson, 1995a). Fault segment linkage in these regions is achieved through breaching of the overstep by a synthetic fault. In the eastern part of the area (Fig. 12), the conjugate faults are highly segmented and few of the segments are linked. Rotated bedding often occurs in the zone between two overstepping fault segments, but through-going faults have not always developed to breach the strike-slip relay ramps (Peacock and Sanderson, 1995a). It should be noted that the strike-slip fault segments rarely overlap to form pull-apart structures. To the west, the faults are less segmented and linkage between the faults is more common.

The distribution of the unconnected faults (Fig. 12 east) is similar to that for the unconnected fault zone at Beadnell (Fig. 6a), whilst the individual conjugate fault zones in the western part of Fig. 12 have some

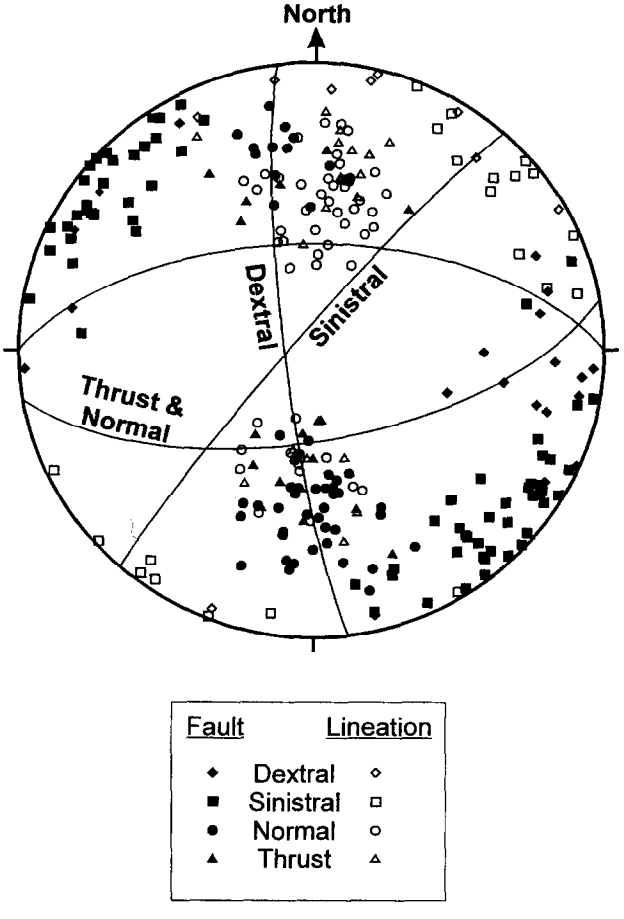

Fig. 10. Equal-area stereogram of poles to planes of dextral (n = 19) and sinistral (n = 66) strike-slip faults; normal faults (n = 53); and thrusts and reverse reactivated normal faults (n = 18) at Kilve, Somerset. Lineation data and great circles are shown to represent the fault planes.

geometrical similarities with the connected network at Beadnell (Fig. 6b).

Table 1 summarises the field observations at both locations.

STRAIN ANALYSIS

The method of Peacock and Sanderson (1993) is used to estimate the magnitudes and orientations of the principal strain axes for each of the described fault zones (Figs 6, 11 & 12). Their approach is based on the displacement-gradient tensor method (Jamison, 1989), but modified to allow fault-strain calculation from a line sample that traverses faults with various orientations. The total fault-strain is derived from the following data for each fault: dip and dip direction, displacement sense, direction and magnitude. The displacement is weighted to account for the angle between the perpendicular to the fault and the sample line, so the estimation of the fault-strain is independent of the line orientation (Peacock and Sanderson, 1993). The weighted displacement-gradient tensor approach provides an ideal method to compare directly fault-strain magnitudes over the two scales of observation.

In the analysis of strain for the networks of conjugate strike-slip faults, the sample lines have been drawn perpendicular to the acute angle bisector of the fault traces (X-X' and Y-Y', Figs 6, 11 & 12), so that their orientations form similar angular relationships with the shortening and extension directions to those of the normal fault set examined by Peacock and Sanderson (1993). The results that are presented are, therefore, derived from an estimation of the summed extension across each fault zone.

The fault-strain analysis of the metre-scale fault zones from Beadnell (Fig. 6) and Kilve (Fig. 11) assumes that all the deformation occurred in the horizontal plane (i.e. plane strain); available slickenside lineation data support this assumption but were not obtainable for all faults. Slickenside lineation data were more widely available for the faults illustrated in Fig. 12, so three-dimensional strain analysis was possible. The displacement-gradient tensor method is an estimation, as the fault-related brittle deformation is approximated to ductile deformation of the strain ellipsoid (or ellipse for two-dimensional analysis) (Jamison, 1989). Moreover, the analysis was carried out for only the master faults on all of the maps. Vein and pull-apart arrays were not included in the analysis of the metre-scale examples, and faults < 1 m long were excluded from the survey of the strike-slip fault network illustrated by the larger-scale map (Fig. 12). A further assumption was made concerning the displacement of the fault at intersection with the sample line. A displacement value was estimated by interpolating between the nearest measured values on either side of the sample line. Unfortunately, this method assumes a linear displacement gradient between the two points, which represents an over-simplification when compared with displacement profiles for individual faults (cf. Williams and Chapman, 1983; Peacock, 1991; Odonne and Massonnat, 1992a).

The deformation in an area must be statistically homogeneous to provide a rigorous strain estimation (Wojtal, 1989; Jamison, 1989), so the sample line

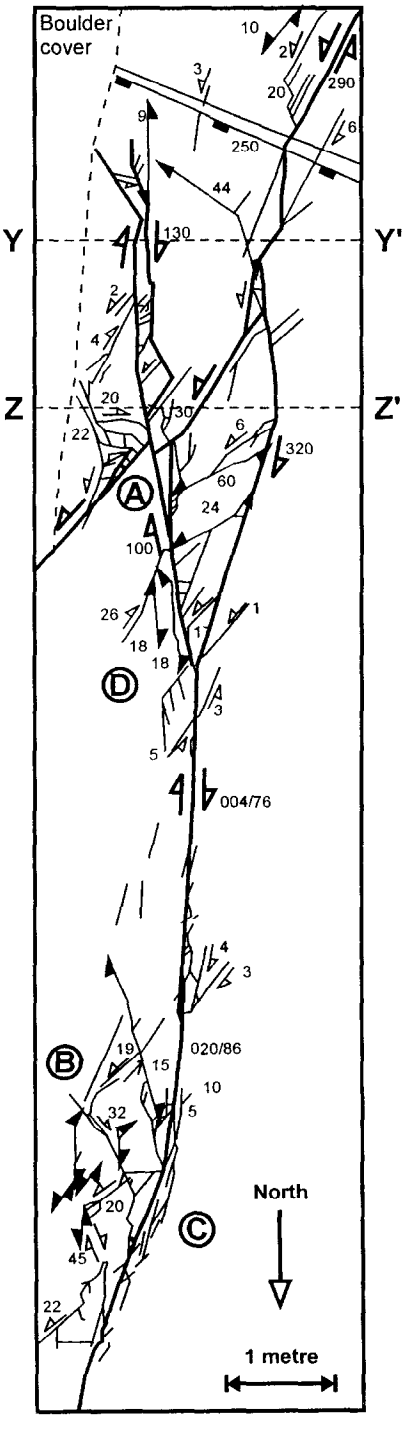

Fig. 11. Conjugate strike-slip fault zone developed in the wall-rock of a 3.5 m maximum displacement dextral strike-slip fault, from Kilve, Somerset (originally mapped at 1:25). Displacements are in mm. See Fig. 6 for key. The circled letters are referred to in the text.

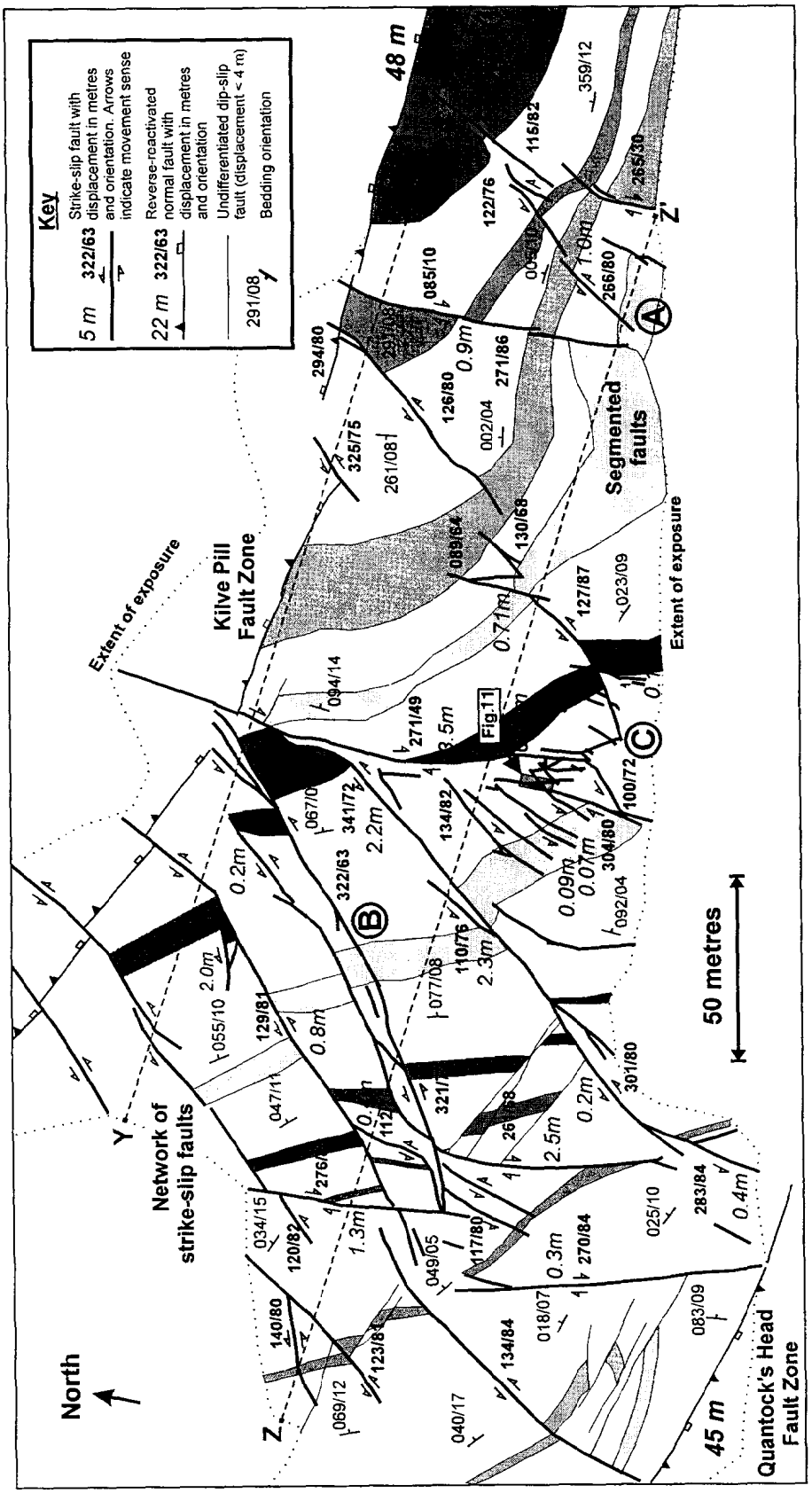

Fig. 12. Map of the strike-slip fault network mapped from aerial photographs at a scale of 1:500. The shaded areas represent individual limestone units. Displacements are in metres. Note the location of Fig. 11.

Table 1. Summary of field observations for Figs 6, 11 and 12. The vein type refers to the classification of Beach (1975): Type 1 = convergent, and Type 2 = bisector parallel. TT = transtension, SS = simple shear and Ext. = extensional. The vein arrays strikes for Fig. 6(a) have been subdivided into dextral (D) and sinistral (S). The dextral and sinistral vein arrays in Fig. 6(b) have similar orientations, so have not been sub-divided

		Fault strikes				Vein		
Figure	Network	Displacement range	Dextral	Sinistral	Arrays	Type	Strikes	Style
6(a)	Unconnected	1–200 mm	ENE–WSW	WNW–ESE	SS–TT	1	D: NE–SW, S: NW–SE	Linear zones
6(b)	Connected	1–500 mm	NE–SW	NW–SE	TT–Ext.	2	ENE–WSW, ESE–WNW	Clustered
11	Connected	1–320 mm	N–S	NE–SW				
12 W	Connected	0.08–3.6 m	N–S	NNE–SSW				
12 E	Unconnected	0.5–1 m	N–S	NE–SW	–			

should be sub-divided if there is considerable heterogeneity (Peacock and Sanderson, 1993). The measured faults in the three metre-scale maps (Figs 6 & 11) are approximately homogeneous, but there is some variation across the larger-scale map (Fig. 12). Cumulative displacement–distance graphs of the faults intersected by the sample lines demonstrate the heterogeneity from east to west of fault spacing and displacement distribution (Fig. 13). The data from the sample line Y–Y' has been sub-divided into two sets, based on the marked shallowing of the slope at approximately 175 m (Fig. 13).

Results

The fault-strain estimates for each of the four maps are shown in Table 2. Fracture densities calculated for each sample line are highly variable, ranging from 0.02 (Y–Y' E, Fig. 12) to 2.27 (Z–Z', Fig. 11) and can be attributed to (1) survey resolution, and (2) the number of measurable faults. All of the faults and veins that were visible to the naked eye were mapped in the metre-scale maps (Figs 6 & 11), but it was not possible to determine the displacement on every fault. On the network of conjugate faults shown in Fig. 12, only faults that were longer than 1 m were mapped, and virtually all displacements were resolvable and included in the analysis. The eigenvalues indicate convincingly that far greater strain was accommodated by the connected networks of strike-slip faults and veins (Figs 6b, 11 & 12 west), than the unconnected examples (Figs 6a & 12 east), even when interpreted in the context of the assumptions.

FAULT ZONE EVOLUTION

It is appropriate to consider the two examples illustrated in Fig. 6, as representing two stages in conjugate fault zone evolution through comparison of the strain analysis and the various structures. The results of the strain analysis (Table 2) indicate that the connected fault zone (Fig. 6b) accommodates far greater strain than the unconnected fault zone (Fig. 6a). It has also been demonstrated by various workers that early fault development occurs through fracture propagation, interaction and subsequent linkage (Gamond, 1983; Cowie and Scholz, 1992; Peacock and Sanderson, 1995b). Intact vein and pull-apart arrays occur in the unconnected fault zone (Fig. 6a), and relics of faulted pull-apart structures occur adjacent to the master faults in the connected fault network (Fig. 6b). The observations of the fault zones at Kilve (Figs 11 & 12) are also incorporated into the model (Fig. 14a–e), on the basis of their geometrical similarities with the maps illustrated in Fig. 6.

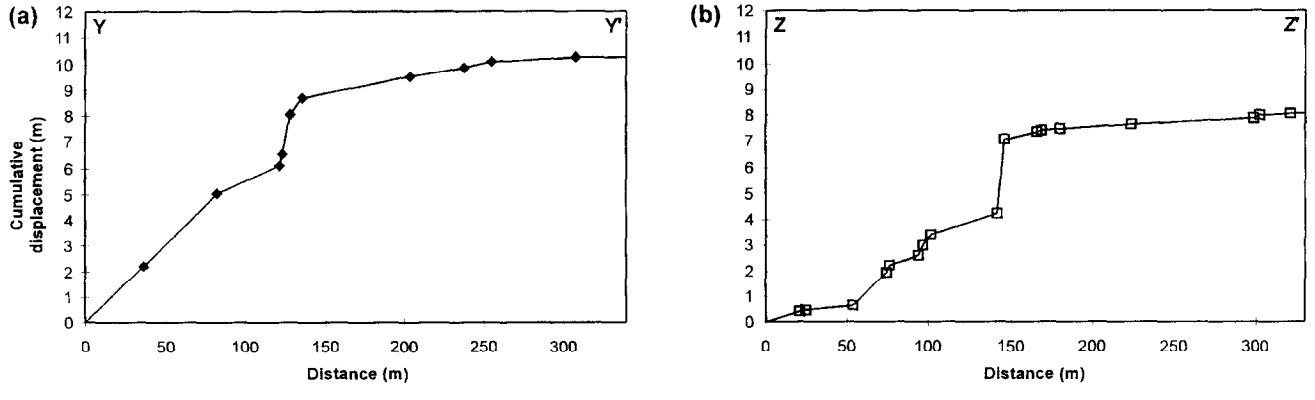

Fig. 13. Cumulative displacement–distance graphs for the two traverses indicated by the dashed lines in Fig. 12. (a) Y–Y', and (b) Z–Z'. The fault that corresponds to the point at which the gradient of the graph in (a) shallows considerably is marked as 'C' in Fig. 12.

Table 2. Results of the strain analysis for sample lines from each of the maps (X–X' and Y–Y', Figs 6, 11 & 12). Data along two sample lines were collected for each map, with the exception of Fig. 6(b) due to insufficient displacement data. e_1 = extension axis, e_3 = shortening axis, and e_2 = intermediate axis (negative = contractional, positive = extensional). The number of faults for each sample line refers to the number of faults with measurable displacement that were included in the analysis, and not the actual number. The extensional and contractional axes orientations (eigenvectors) are indicated by the arrows in the final column (north is at the top of the page)

Figure	Line	Length (m)	Number of faults	Density (Nm^{-1})	Eigenvalues (2sf) e_1	e_2	e_3	Strain axes
6(a)	Y–Y'	15.2	4	0.26	0.0089	—	−0.0089	
	Z–Z'	15.2	4	0.26	0.0099	—	−0.0099	
6(b)	Y–Y'	14.8	6	0.41	0.038	—	−0.038	
11	Y–Y'	2.63	4	1.52	0.043	—	−0.043	
	Z–Z'	2.63	6	2.28	0.063	—	−0.063	
12	Y–Y'	313.3	10	0.03	0.026	0.00062	−0.026	
	E	138.3	4	0.02	0.00063	−0.00007	−0.0062	
	W	175.0	6	0.04	0.047	−0.0017	−0.048	
	Z–Z'	338.7	17	0.05	0.020	0.00069	−0.024	
	E	163.7	4	0.03	0.0037	0	−0.0026	
	W	175.0	13	0.06	0.031	0.0011	−0.038	

Faults and vein arrays in the unconnected fault zone illustrated in Fig. 6(a) are preserved in various stages of development, such that there are (1) en échelon vein and pull-apart arrays, (2) fault segments with irregular traces that are co-linear with vein arrays, (3) fault segments 'linked' by en échelon vein arrays, and (4) contractional and extensional oversteps along master faults, but there are no conjugate intersection points between faults. The presence of this range of structures suggests that different parts of the rock deformed at different rates, but a lack of cross-cutting structures implies that these processes occurred during a single progressive event.

The Type 1 veins depicted in Fig. 6(a) form densely populated linear zones at fault-tips, and also form shear zones that are antithetic to master faults. Type 1 veins commonly occur in existing shear zones (Beach, 1975; Rothery, 1988), and localisation into linear zones may form at the periphery of a parent fracture (Pollard *et al.*, 1982; Cruickshank *et al.*, 1991). Type 2 veins are more commonly associated with vein arrays in extensional regimes (e.g. Beach, 1975; Rothery, 1988), but the Type 2 veins in Fig. 6(a) have vein-zone angles that indicate extensional to simple shear deformation. The model of Olson and Pollard (1991) may be applicable, whereby sub-parallel fractures are able to grow and interact during a single episode of extension to produce arrays with geometries that range from extensional to transpressional. The arrays can then serve to localise subsequent shear (Beach, 1975; Pollard *et al.*, 1982; Rothery, 1988; Olson and Pollard, 1991). An alternative explanation for the presence of the Type 2 veins at A (Fig. 6a) is that they occur in a tensional quadrant adjacent to the tip of a master fault (e.g. Cruickshank *et al.*, 1991) and represent a fault-tip damage zone (McGrath and Davison, 1995). A similar mode of formation, however, is not applicable to the veins in the antithetic arrays adjacent to B (Fig. 6b).

A sub-division of the veins into separate deformation events can be based on their orientations and interpreted formation mechanism.

Stage 1—Extensional vein development

The model of Olson and Pollard (1991) is appropriate to describe the initial formation of sub-parallel Type 2 veins in the rock mass that form into arbitrarily orientated arrays during effective extension (Fig. 14a & f). These veins are interpreted as the first-formed structures as they were able to grow as sub-parallel extension fractures, and their orientations or geometries were not modified significantly by interaction with other structures or in shear zones.

Stage 2—Formation of conjugate strike-slip faults

Two possible mechanisms to describe the formation of conjugate faults at low angles (i.e. $\ll 60°$) to each other (cf. Hancock, 1985) (Fig. 6a) are (1) coalescence of the Stage 1 vein arrays during continued growth, followed by shear, or (2) shear deformation localised onto the pre-existing extensional veins. The Type 1

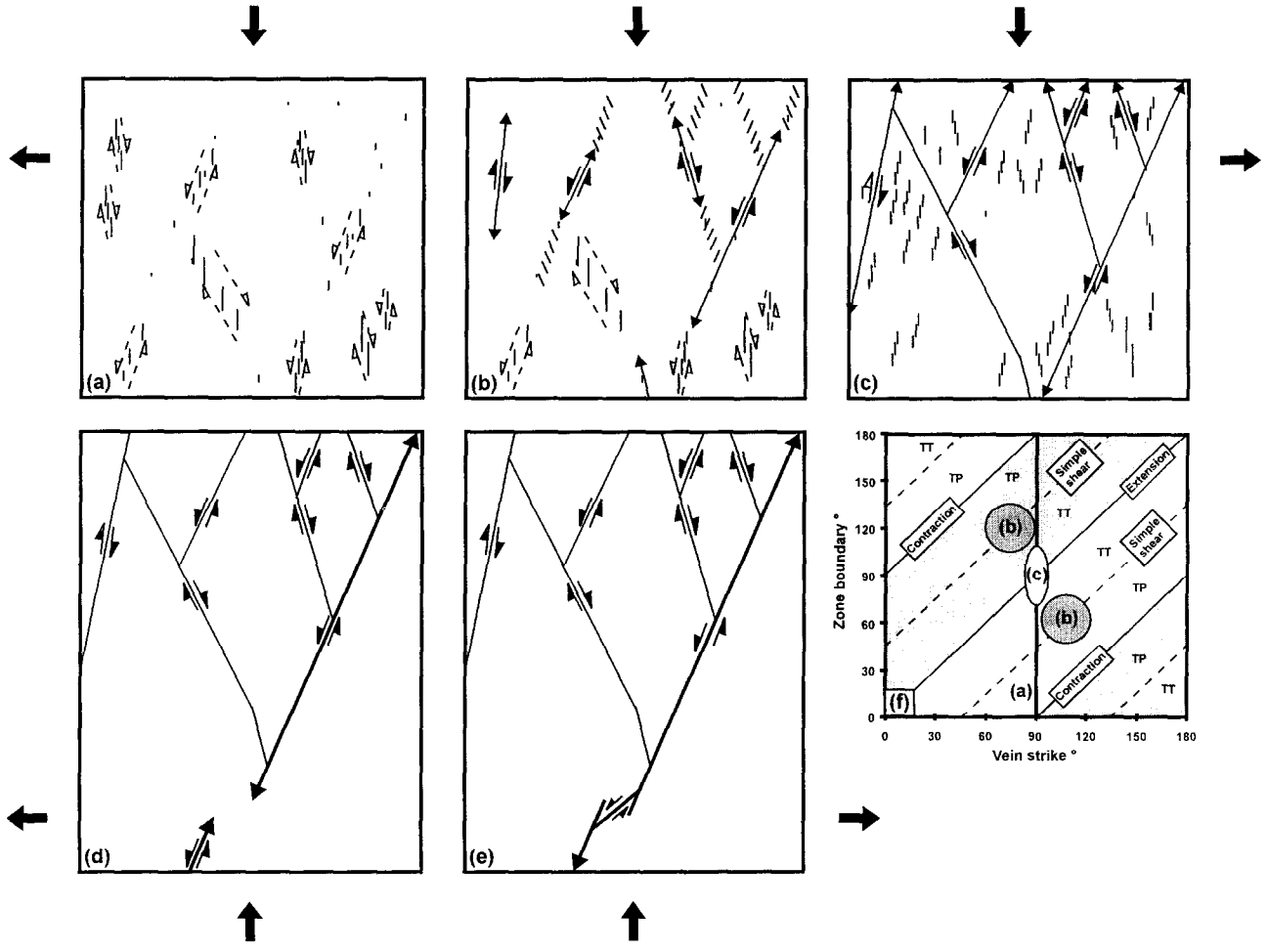

Fig. 14. Model for the development of strike-slip fault zones to include conjugate fault development and overstepping zones. The arrowed faults indicate those parts active at that particular stage. (a) (c) Models based on observations at Beadnell. (d) (e) Expansion of the model to include the observations of fault network development at Kilve. The model is discussed in full in the text. (f) Idealised graph of vein strike and zone boundary orientation for (a) (c) (cf. Fig. 7). Veins in (a) are parallel to each other, but there is the potential for the zone boundaries to have the whole range of orientations. The data from (b) plot in two distinct clusters that represent Type 1 veins within arrays with predominantly simple shear geometries. The data from the natural examples (Fig. 6) show some overlap in vein strike of the two clusters. The veins in (c) are sub-parallel within the transtensional extensional arrays, and the spread of zone boundary orientations is limited, so the data plot in a single cluster. Veins with transtensional extensional geometries were not observed within the fault zones at Kilve.

vein geometries (Fig. 6a) indicate that simple shear deformation was an important process (Beach, 1975; Rothery, 1988), and occurrence of veins at high angles adjacent to the master faults provides evidence that the strike-slip faults formed from arrays with simple shear geometries (Fig. 14b & f). A three-dimensional view of the strike-slip fault network was not possible, so conclusions cannot be drawn to explain the localisation into linear zones of the vein arrays with simple shear geometries (cf. Cruickshank *et al.*, 1991). The interpretation of the deformation shown in Fig. 6(a) involves several conjugate systems (of faults and veins) being active at a similar time (cf. Nicol *et al.*, 1995) before linking to produce master faults (Fig. 14b). Analysis of the fault locations demonstrates that they propagate towards intersection points, and never initiate at them (Fig. 6a).

Stage 3—Fault linkage and renewed extensional vein opening

Conjugate faults with similar displacement magnitudes lock at an intersection, and propagation continues away from this point (Fig. 14c) (cf. Peacock, 1991). The propagation direction of faults is evident from vein distributions along-side the master faults, with microcracks forming asymmetrically about a Mode II fracture tip (Reches and Lockner, 1994) (Fig. 1). Extensional fractures initiate at flaws in the rock (Olson and Pollard, 1991), so new veins that initiated in the wake of a process zone would have an

asymmetric distribution (e.g. at B and C, Fig. 6b). Smaller faults that propagate towards the master fault become stuck at their intersection, and there are no examples of breached intersections in the linked fault zone (Fig. 6b). The network continues to develop and link with the initiation and propagation of new faults.

Type 2 veins in the connected fault zone (Fig. 6b) differ from Type 2 veins in Fig. 6(a) in that they form arrays with predominantly extensional geometries, and the vein-zone angles do not vary significantly (Figs 7a & 14f). Formation of these veins before Stage 3 can be discounted due to the lack of (1) any cross-cutting structures, (2) evidence of subsequent shear failure and (3) similar structures in Fig. 6(a) (but there are through-faulted Type 1 veins in Fig. 6b). Prior to their intersection, the strike-slip faults are able to grow unhindered, so extension across the zone is possible through shear failure along existing faults and Type 1 vein arrays. Vein arrays with predominantly extensional geometries (Figs 6b & 8b) must have developed, therefore, after the establishment of a linked fault network (Fig. 14c).

The important results from the two very different networks (Fig. 6) are that the style of veining changed systematically during conjugate strike-slip fault zone development (Fig. 14a–c & f). An initial phase of subparallel vein formation during an extensional phase pre-dates shear failure (Fig. 14a). Shear deformation then dominates with the formation of co-linear vein arrays with simple shear geometries that are subsequently breached to form strike-slip faults (Fig. 14b) (cf. Peacock and Sanderson, 1995b, Willemse *et al.*, 1997). After the establishment of a connected fault network, all the simple shear is accommodated by movement concentrated on the linked network of strike-slip faults, but the unfaulted rock mass is able to fail further through the development of extensional vein arrays (Fig. 14c). There is therefore a progression from (1) development of Type 2 veins from randomly distributed microcracks, through (2) Type 1 vein development (Mode I failure) within simple shear vein arrays concentrated in linear zones (Fig. 6a), to (3) the formation of and shear across a linked network of strike-slip faults (Mode II), and finally (4) a renewed phase of Type 2 vein arrays with extensional geometries (Fig. 6b). The sole major difference between the examples in the two locations is that vein arrays with these geometries were not observed in the fault zones at Kilve (Figs 11 & 12).

Stage 4—Breaching of the intersection points

The next two stages of fault zone development are based on the geometries of the fault zones examined at Kilve, where intersection points are often breached (Figs 11 & 12). In the metre-scale example (Fig. 11), the master sinistral fault first breached the sticking point, but is in turn offset by the dominant dextral fault that effectively by-passes the conjugate set. The offset of the sinistral fault by the dextral fault and a lack of evidence of pressure solution at the intersection point (Fig. 11) indicate sequential rather than synchronous fault activity (Odonne and Massonnat, 1992a), and the map shown in Fig. 11 implies that one fault became increasingly important during the later stages of development. In the model presented here, the sinistral fault breaches the overstep and continued to propagate in both directions (Fig. 14d).

Stage 5—Linkage with other fault systems

In the final stage, the dominant fault continues to propagate in both directions, and eventually oversteps with another propagating fault segment. The overstep region is eventually broken through by a linking, synthetic fault at a strike-slip relay ramp (Fig. 14e) (Peacock and Sanderson, 1995a). Minor antithetic faults and relics of strike-slip relay ramps are often preserved along-side the through-going faults (Peacock and Sanderson, 1995a) (Fig. 14e). The occurrence of a conjugate network of strike-slip faults on the inside of the bend (at B, Fig. 11) can be attributed to two factors: (1) a contractional bend that would indicate that this part of the fault propagated southwards (Sibson, 1989), which is supported by subsidiary fractures on the opposite side of the fault (at C), or (2) a conjugate strike-slip fault zone that formed prior to the development of the master fault and was subsequently by-passed (see below). The damage at 'D' implies that this segment was propagating northwards, and the probable linkage point between these two segments is at the branch-point of the fault adjacent to 'B'. A large fault network (Fig. 12) evolves from the continuing development, propagation and linkage of fault segments. The sinistral faults dominate the foreshore, and segment linkage has been observed on several trace-length scales from the millimetre-scale to the 100 metre-scale. Linkage between the larger faults and compartmentalisation of the rock mass are rare during the early stages of development, but increase as faults breach the oversteps. The geometry of the active part of a fault zone simplifies with time as these heterogeneities are by-passed by single dominant faults (Figs 11 & 12).

CONCLUSIONS

1. This paper describes the geometry and evolution of conjugate strike-slip fault zones in limestones, and shows that deformation becomes concentrated on the largest faults. Metre-scale examples are described in detail, which have similar geometries to larger fault networks.

2. Strain analysis indicates that far greater strains are accommodated by connected, rather than unconnected, networks of conjugate strike-slip faults.
3. The geometries of metre-scale strike-slip fault zones indicate the following stages of development (Fig. 14). (a) Opening of dilational veins during extension. (b) The subsequent processes that contribute to the formation of strike-slip networks (simple shear vein array initiation and fault development) indicate strain accommodation at different rates in different areas of the fault zone. Conjugate sets of unlinked strike-slip faults develop in isolation and propagate towards intersection points. (c) Once a linked network of faults is established, deformation is accommodated largely by slip on the master fault, with new vein arrays developing with predominantly extensional geometries. (d) Intersection points are breached by dominant faults. (e) The geometry of the active fault system simplifies after conjugate intersection points are breached and the complexities become inactive and are by-passed. By-passed portions remain preserved in the walls of the master faults.

Acknowledgements— Funding for this work was partly provided by Elf Aquitaine, through Keith Rawnsley. PGK is grateful for the support of a research studentship from the University of Southampton. An anonymous reviewer, R. Myers and R. Norris are thanked for their constructive comments and criticisms that greatly improved an earlier version of the manuscript.

REFERENCES

Angelier, J. (1984) Tectonic analysis of fault slip data sets. *Journal of Geophysical Research* **89,** 5835–5848.

Aydin, A. and Nur, A. (1982) Evolution of pull-apart basins and their scale independence. *Tectonics* **1,** 91–105.

Beach, A. (1975) The geometry of en-échelon vein arrays. *Tectonophysics* **28,** 245–263.

Benard, F., Mascle, A., Le Gall, B., Dogligez, B. and Rossi, T. (1990) Palaeo-stress fields in the Variscan foreland during the Carboniferous from microstructural analysis in the British Isles. *Tectonophysics* **177,** 1–13.

Bowyer, M. O'N. and Kelly, P. G. (1995) Strain and scaling relationships of faults and veins at Kilve, Somerset, UK. *Proceedings of the Ussher Society* **8,** 411–415.

Brooks, M., Trayner, P. M. and Trimble, T. J. (1988) Mesozoic reactivation of Variscan thrusting in the Bristol Channel area, UK. *Journal of the Geological Society of London* **145,** 439–444.

Chadwick, R. A. (1986) Extension tectonics in the Wessex Basin, southern England. *Journal of the Geological Society of London* **143,** 444–465.

Chester, F. M. and Logan, J. M. (1986) Implications for mechanical properties of brittle faults from observations of the Punchbowl Fault Zone, California. *Pure and Applied Geophysics* **124,** 79–106.

Collier, R. E. Ll. (1989) Tectonic evolution of the Northumberland Basin: the effects of renewed extension upon an inverted extensional basin. *Journal of Geological Society of London* **146,** 981–989.

Cowie, P. A. and Scholz, C. H. (1992) Physical explanation for the displacement–length relationship of faults using a post-yield fracture mechanics model. *Journal of Structural Geology* **14,** 1133–1148.

Cruickshank, K. M., Zhao, G. and Johnson, A. M. (1991) Analysis of minor fractures associated with joints and faulted joints. *Journal of Structural Geology* **13,** 865–886.

Freund, R. (1974) Kinematics of transform and transcurrent faults. *Tectonophysics* **21,** 93–134.

Gamond, J. F. (1983) Displacement features associated with fault zones: a comparison between observed examples and experimental models. *Journal of Structural Geology* **5,** 33–45.

Hancock, P. L. (1985) Brittle microtectonics: principles and practices. *Journal of Structural Geology* **7,** 437–457.

Hempton, M. R. and Dunne, L. A. (1984) Sedimentation in pull-apart basins: active examples in eastern Turkey. *Journal of Geology* **92,** 513–530.

Horsfield, W. T. (1980) Contemporaneous movement along crossing conjugate normal faults. *Journal of Structural Geology* **2,** 305–310.

Jamison, W. R. (1989) Fault-fracture strain in Wingate Sandstone. *Journal of Structural Geology* **11,** 959–974.

Knott, S. D., Beach, A., Brockbank, P. J., Brown, J. L., McCallum, J. E. and Welbon, A. I. (1996) Spatial and mechanical controls on normal fault populations. *Journal of Structural Geology* **18,** 359–372.

Lake, S. D. and Karner, G. D. (1987) The structure and evolution of the Wessex Basin, southern England: an example of inversion tectonics. *Tectonophysics* **137,** 347–378.

Mann, P., Hempton, M. R., Bradley, D. C. and Burke, K. (1983) Development of pull-apart basins. *Journal of Geology* **91,** 529–554.

McCoss, A. (1986) Simple constructions for deformation in transpression/transtension zones. *Journal of Structural Geology* **8,** 715–718.

McGrath, A. G. and Davison, I. (1995) Damage zone geometry around fault tips. *Journal of Structural Geology* **17,** 1011–1023.

Nicol, A., Walsh, J. J., Watterson, J. and Bretan, P. G. (1995) Three-dimensional geometry and growth of conjugate normal faults. *Journal of Structural Geology* **17,** 847–862.

Odonne, F. and Massonnat, G. (1992a) Compatibility of strain and displacement around simple and conjugate faults, analog models of natural structures. *Bulletin de la Societe Geologique de France* **163,** 701–712.

Odonne, F. and Massonnat, G. (1992b) Volume loss and deformation around conjugate fractures—comparison between a natural example and analog experiments. *Journal of Structural Geology* **14,** 963–972.

Olson, J. E. and Pollard, D. D. (1991) The initiation and growth of en échelon veins. *Journal of Structural Geology* **13,** 595–608.

Peacock, D. C. P. (1991) Displacement and segment linkage in strike-slip fault zones. *Journal of Structural Geology* **13,** 1025–1035.

Peacock, D. C. P. and Sanderson, D. J. (1991) Displacements, segment linkage and relay ramps in normal fault zones. *Journal of Structural Geology* **13,** 721–733.

Peacock, D. C. P. and Sanderson, D. J. (1992) Effects of layering and anisotropy on fault geometry. *Journal of the Geological Society of London* **149,** 793–802.

Peacock, D. C. P. and Sanderson, D. J. (1993) Estimating strain from fault slip using a line sample. *Journal of Structural Geology* **15,** 1513–1516.

Peacock, D. C. P. and Sanderson, D. J. (1995a) Strike-slip relay ramps. *Journal of Structural Geology* **17,** 1351–1360.

Peacock, D. C. P. and Sanderson, D. J. (1995b) Pull-aparts, shear fractures and pressure solution. *Tectonophysics* **241,** 1–13.

Peacock, D. C. P. and Zhang, X. (1994) Field examples and numerical modelling of oversteps and bends along normal faults in cross-section. *Tectonophysics* **234,** 147–167.

Pollard, D. D., Segall, P. and Delaney, P. T. (1982) Formation and interpretation of dilatant échelon cracks. *Geological Society of America Bulletin* **93,** 1291–1303.

Reches, Z. and Lockner, D. A. (1994) Nucleation and growth of faults in brittle rocks. *Journal of Geophysical Research* **99,** 18,159–18,173.

Robson, D. A. (1977) The structural history of the Cheviot and adjacent regions. *Scottish Journal of Geology* **13,** 255–262.

Rothery, E. (1988) En-échelon vein array development in extension and shear. *Journal of Structural Geology* **10,** 63–71.

Sanderson, D. J. and Marchini, W. R. D. (1984) Transpression. *Journal of Structural Geology* **6,** 449–458.

Scholz, C. H., Dawers, N. H., Yu, J.-Z. and Anders, M. H. (1993) Fault growth and fault scaling laws: preliminary results. *Journal of Geophysical Research* **98,** 21,951–21,961.

Segall, P. and Pollard, D. D. (1980) Mechanics of discontinuous faults. *Journal of Geophysical Research* **85,** 4337–4350.

Shiells, K. A. G. (1964) The geological structure of north-east Northumberland. *Transactions of the Royal Society of Edinburgh* **65,** 449–481.

Sibson, R. H. (1989) Earthquake faulting as a structural process. *Journal of Structural Geology* **11,** 1–14.

Stauffer, D. and Aharony, A. (1992) *Introduction to Percolation Theory*, Taylor and Francis, London.

Whittaker, A. and Green, G. W. (1983) *Geology of the county around Weston-super-Mare*. Geological Survey of Great Britain.

Willemse, E. J. M., Peacock, D. C. P. and Aydin, A. (1997) Nucleation and growth of strike-slip faults in limestone. *Journal of Structural Geology* **19,** 1461–1477.

Williams, G. D. and Chapman, T. (1983) Strains developed in the hangingwalls of thrusts due to their slip/propagation rate: a dislocation model. *Journal of Structural Geology* **9,** 563–571.

Wojtal, S. (1989) Measuring displacement gradients and strains in faulted rocks. *Journal of Structural Geology* **11,** 669–678.